THE JOURNAL OF BIOLOGICAL CHEMISTRY VOL. 285, NO. 18, pp. 13490–13497, April 30, 2010
© 2010 by The American Society for Biochemistry and Molecular Biology, Inc. Printed in the U.S.A.

The Transmembrane Domains of L-selectin and CD44 Regulate Receptor Cell Surface Positioning and Leukocyte Adhesion under Flow*

Received for publication, January 9, 2010, and in revised form, March 2, 2010 Published, JBC Papers in Press, March 8, 2010, DOI 10.1074/jbc.M110.102640

Konrad Buscher[‡§], Sebastian B. Riese[‡], Mehdi Shakibaei[¶], Christian Reich[‡‖], Jens Dernedde[‡], Rudolf Tauber[‡1], and Klaus Ley[§1,2]

From the [‡]Central Department of Laboratory Medicine and Pathobiochemistry and the [‖]Department of Anesthesiology and Intensive Care Medicine, Charité-Universitätsmedizin, 10117 Berlin, Germany, the [¶]Department of Anatomy, Ludwig Maximilians University, 80539 Munich, Germany, and the [§]Division of Inflammation Biology, La Jolla Institute for Allergy and Immunology, La Jolla, California 92037

During inflammation and immune surveillance, initial contacts (tethering) between free-flowing leukocytes and the endothelium are vitally dependent on the presentation of the adhesion receptor L-selectin on leukocyte microvilli. Determinants that regulate receptor targeting to microvilli are, however, largely elusive. Therefore, we systematically swapped the extracellular (EC), transmembrane (TM), and intracellular (IC) domains of L-selectin and CD44, a hyaluronan receptor expressed on the cell body and excluded from microvilli. Electron microscopy of transfected human myeloid K562 cells showed that the highly conserved TM domains are responsible for surface positioning. The TM segment of L-selectin forced chimeric molecules to microvilli, and the CD44 TM domain evoked expression on the cell body, whereas the IC and EC domains hardly influenced surface localization. Transfectants with microvillus-based chimeras showed a significantly higher adhesion rate under flow but not under static conditions compared with cells with cell body-expressed receptors. Substitution of the IC domain of L-selectin caused diminished tethering but no change in surface distribution, indicating that both microvillus positioning and cytoskeletal anchoring contribute to leukocyte tethering. These findings demonstrate that TM domains of L-selectin and CD44 play a crucial role in cell adhesion under flow by targeting receptors to microvilli or the cell body, respectively.

Neutrophil invasion at sites of inflammation as well as lymphocyte recirculation from blood into secondary lymphoid tissue require that free-flowing leukocytes become activated and subsequently exit the bloodstream. At the molecular level, the cells undergo a closely orchestrated cascade of interactions with the endothelium, each step consisting of a characteristic pattern of receptors, their ligands, cytokines, and chemoattractants (1, 2).

Distinct cell surface receptor segregation is a widely observed phenomenon with effects on cell proliferation, migration, and tumorigenesis (3). Leukocyte membrane protrusions known as microvilli serve as active grouping sites for a variety of surface receptors including L-selectin (4), α4-integrins (5), P-selectin glycoprotein ligand 1 (PSGL-1)[3] (6, 7), CD4, and the chemokine receptors CCR5 and CXCR4 (8). In contrast, the hyaluronan receptor CD44 (4) and the integrins $\alpha M\beta 2$ (Mac-1) and $\alpha L\beta 2$ (LFA-1) (9, 10) show expression on the planar cell body excluding microvilli.

Both L-selectin and CD44 are type I integral membrane glycoproteins expressed on most circulating leukocytes. L-selectin knock-out mice show a profound defect of lymphocyte accumulation in secondary lymphatic tissue and of neutrophils at sites of inflammation (11). CD44 is involved in many physiological processes, including lymphocyte activation, adhesion, and proliferation (12). There is also increasing evidence that CD44 and L-selectin contribute to tumor metastasis (13, 14).

Under many physiologic conditions, L-selectin initiates the first step of the adhesion cascade (15, 16). While surveying the vascular bed, rapidly flowing leukocytes face the challenge to establish contact to static ligands of the endothelial layer at high velocities. Presentation of adhesion receptors on microvilli as the very distal aspects of the cell may be a functional adaptation to facilitate adhesion under high shear stress. Indeed, L-selectin transfectants in murine pre-B cells showed impaired tethering capability under flow when expressed on the cell body using a chimera consisting of the ectodomain of L-selectin linked to CD44 (4). This concept was further confirmed by adhesion assays using the same transfectants in lymphoid tissue *in vivo* (17). These studies established a close relationship between receptor surface topography and function, thus attaching great importance to the microvillus compartment in the context of leukocyte recruitment.

Although leukocyte surface structures including microvilli, ruffles, filopodia, and lamellipodia are well described (18), a detailed biochemical understanding of their receptor composi-

* This work was supported, in whole or in part, by National Institutes of Health Grant EB 02185. This work was also supported by Deutsche Forschungsgemeinschaft Grant Sonderforschungsbereich 449 and Boehringer Ingelheim Fonds.

[1] Both authors share senior authorship.

[2] To whom correspondence should be addressed: Division of Inflammation Biology, La Jolla Institute for Allergy and Immunology, 9420 Athena Circle Dr., La Jolla, CA 92037. Tel.: 858-752-6661; Fax: 858-752-6986; E-mail: klaus@liai.org.

[3] The abbreviations used are: PSGL-1, P-selectin glycoprotein ligand 1; ERM, ezrin/radixin/moesin; IC, intracellular; EC, extracellular; TM, transmembrane; mAb, monoclonal antibody.

Downloaded from www.jbc.org at Biomedical Library, UCSD, on September 30, 2010

tion is still largely missing. To date, it is well recognized that cytoplasmic interactions can regulate protein sorting (19). L-selectin distribution on microvilli is abolished upon mutation of its intracellular ezrin/radixin/moesin (ERM) binding site (20). The tail-truncated L-selectin mutant LΔcyto containing only the membrane-proximal ERM binding site of the intracellular (IC) domain still localizes to microvilli (21). As a consequence, cytoskeletal linkage to ERM is commonly believed to be a main determinant of surface localization. However, CD44 links to ERM proteins, too (22), yet shows an inverse surface expression pattern on nonprotrusive sections. Hence, definitive roles for protein domains in trafficking receptors to or away from microvilli have not been established. To investigate the process and implications of receptor segregation on leukocytes, we conducted domain swapping studies between L-selectin (microvilli) and CD44 (cell body) and evaluated the separate contributions of their extracellular (EC), transmembrane (TM), and IC domains on ultrastructural receptor localization and receptor functionality. Surprisingly, we found that the membrane-spanning domain contains the entire recognition pattern for specific receptor surface segregation on microvilli or the cell body, which in turn crucially affected the efficiency of leukocyte adhesion under flow.

MATERIALS AND METHODS

Antibodies and Reagents—The high fidelity Phusion Polymerase (Finnzyme, Espo, Finland) was used for generating recombinant DNA. Flow cytometry and cell-sorting samples were stained with mouse anti-human CD62L (DREG-56) and mouse anti-human CD44 mAb (clone 515) conjugated with R-phycoerythrin. IgG_1 κ-phycoerythrin served as isotype control. All flow cytometry antibodies were purchased from BD Biosciences. For immunolabeling, mouse anti-human CD62L mAb (DREG-55, provided by E. C. Butcher, Stanford University, Stanford, CA) and goat anti-mouse gold-labeled 10-nm IgG(Fc) antibodies (GE Healthcare) were used. The flow chamber was coated with PSGL-1-Fc (R&D Systems) or hyaluronan from rooster comb (Sigma-Aldrich). Notably, commercial preparations of hyaluronan might also contain chondroitin sulfate as another ligand for CD44. For blocking experiments, anti-L-selectin mAb DREG-200 (provided by E. C. Butcher) (23) and anti-CD44 mAb clone 515 (BD Biosciences) (24, 25) were used.

Recombinant DNA—Full-length cDNA of human L-selectin and CD44 was used as template for domain swapping employing a splicing by overlap extension PCR protocol (26). In brief, the desired gene region, either only the IC or in combination with the TM domain, were amplified using primers that include an overlap extension site. A second PCR step then allowed linkage of the amplificate to the respective ectodomain. All constructs were subcloned into the eukaryotic vector pIRES2-EGFP (Clontech, Mountain View, CA) containing a cytomegalovirus promoter. Nucleotide sequence authenticity was verified by DNA sequencing.

Cell Culture and Transfection—K562 human myeloid leukemia cells (CCL 243, American Type Culture Collection, Rockville, MD) were transfected by electroporation and cultured according to standard protocols. Cell transfectants were sorted on a FACSAria cell sorter (Becton Dickinson) and resorted periodically. This cell line was chosen because it does not express either endogenous CD44 or L-selectin. Preliminary data regarding microvillus positioning of CD44, L-selectin and the chimera LCL were also obtained using the human pre-B cell line Nalm-6 (data not shown).

Flow Cytometry and Immunoelectron Microscopy—Cells were fluorescently labeled using a standard protocol and analyzed on a FACSCalibur flow cytometer (BD Biosciences). The pre-embedding immunolabeling technique has been described previously (27). Briefly, 2×10^6 cells were incubated with the primary antibody at a dilution of 1:10 in phosphate-buffered saline + 1% fetal calf serum at 4 °C for 10 min. The secondary antibody conjugated to 10-nm gold particles was added at a dilution of 1:30 for 10 min at 4 °C followed by fixation and dehydration. Thin sections were cut on a Reichert Ultracut microtome and stained with 2% uranyl acetate and 2% lead citrate. Images were taken using a Zeiss EM10 microscope. Analysis of the 10-nm colloidal gold distribution was performed by a blinded observer at a magnification of ×30,000–60,000. For each transfectant, 20–30 cells were analyzed with a total of 700–1,400 particles. A mock transfectant as negative control did not show any staining.

Static Adhesion assay—Hydrophobic glass slides were coated with 2 mg/ml hyaluronan or 30 μg/ml PSGL-1 and blocked with bovine serum albumin. A 10-ml cell suspension (5×10^6 cells/ml, Hanks' balanced salt solution medium for L-selectin, RPMI 1640 medium for CD44) was added and incubated at 37 °C for 15 min. The number of adhesive cells was assessed with an inverted microscope Zeiss Axio 100. Cells incubated with 10 μg/ml blocking mAb for 10 min at 37 °C were used as controls.

Adhesion Assays under Flow—Adhesion under flow was investigated using a parallel plate flow chamber from GlycoTech (Gaithersburg, MD) placed on a 35-mm polystyrene dish and connected to a high precision perfusion pump (Harvard Apparatus, Holliston, MA). An inverted microscope Axio 100 (Zeiss, Jena, Germany) was used at ×10 magnification equipped with the digital high performance camera SensiCam QE (Cooke Corporation, Romulus, MI). As a specificity control, cells were incubated for 10 min at 37 °C with 10 μg/ml blocking antibody prior to the experiment.

L-selectin Rolling on PSGL-1—Each dish was coated with 150 μg/ml recombinant PSGL-1-Fc for 2 h and then blocked with 2 mg/ml bovine serum albumin for 1 h. Cells were resuspended in Hanks' balanced salt solution containing 1.26 mM Ca^{2+} (Lonza, Basel, Switzerland) with a final concentration of 1×10^6 cells/ml. Rolling assays were started at 2.3 dynes/cm^2, and shear stress was gradually decreased to 1.7, 1.3, and 0.7 dynes/cm^2. Three different fields of view were recorded for a duration of 20 s and extrapolated to 1 min. Velocity determination was performed using a MATLAB (version 7.5.0, R2007B) cell tracking software by John Pickard.

CD44 Adhesion on Hyaluronan—Soluble hyaluronan was plated at 2.0 mg/ml in phosphate-buffered saline, incubated overnight at 37 °C, and subsequently blocked with 2 mg/ml bovine serum albumin in phosphate-buffered saline for 1 h. Cells (1×10^6/ml) were washed and resuspended in RPMI 1640

Downloaded from www.jbc.org at Biomedical Library, UCSD, on September 30, 2010

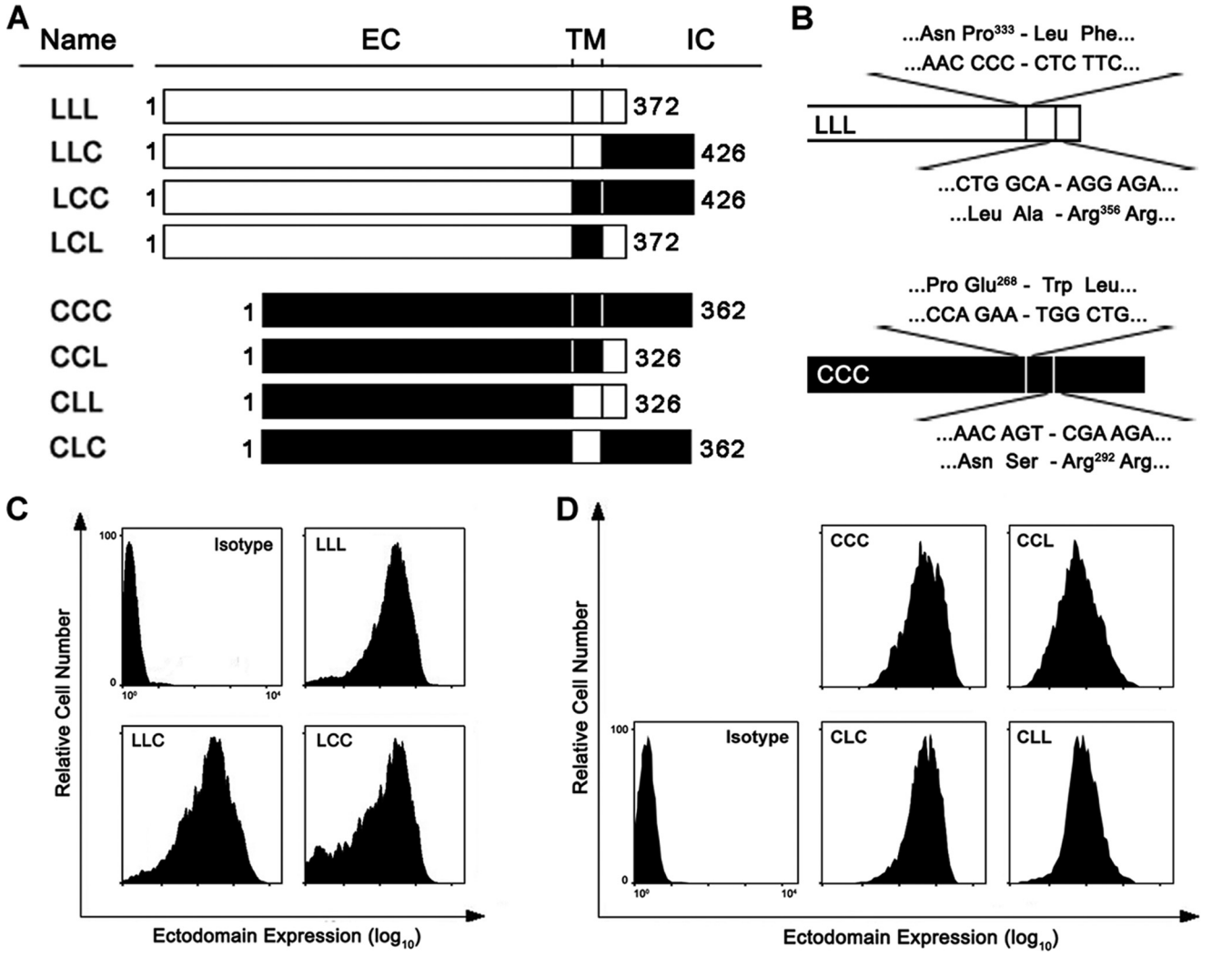

FIGURE 1. **Domain-swapped receptors.** *A*, schematic representation of human wild type L-selectin (LLL, *white*), CD44 (CCC, *black*) and all domain chimeras. The *first*, *second*, and *third letters* denote the EC, TM, and IC domains, respectively. *Numbers* next to the *bars* indicate amino acids starting at the mature N terminus. *Bars* are drawn to scale. *B*, amino acid and nucleotide splicing sites at the domain transitions used for domain swapping. *C* and *D*, FACS histograms showing matched expression levels of three of the four L-selectin (LCL was expressed at lower levels; data not shown) and all CD44 transfectants after cell sorting stained with anti-human fluorescence-labeled mAbs or isotype IgG_1. Only clones with similar surface expression levels were used for functional analysis.

medium. After 7 min of flow, pictures of three different fields of view were taken.

RESULTS

The Intracellular Tail Is Not Sufficient for Defining Receptor Surface Topology—L-selectin (CD62L) and CD44 show a clearly distinct cell surface topology on microvilli and the cell body, respectively. Because published data mainly emphasize cytoplasmic interactions in determining surface positioning, we first set out to address the question of whether the IC domains of L-selectin and CD44 affect compartmentalized surface distribution.

We generated domain-swapped chimeras between the cytoplasmic domains of human L-selectin and CD44 (Fig. 1, *A* and *B*), referred to by a three-letter code, each letter representing a protein domain starting at the N-(extracellular) and ending at the C terminus (intracellular). The human myeloid cell line K562 (L-selectin- and CD44-negative) was stably transfected, and successful expression was verified by flow cytometry (Fig. 1, *C* and *D*) and SDS-PAGE (data not shown). The surface topography of wild type and swapped receptors transfected into myeloid cells was then assessed by immunogold labeling and transmission electron microscopy. No morphologic difference of the microvillus architecture was observed among the transfectants.

Consistent with previous findings (4), 88% of L-selectin (LLL) was associated with microvilli, whereas CD44 (CCC) concentrated on the planar cell body. Surprisingly, the substitution of either cytoplasmic tail did not have significant effects on surface topology. LLC was still positioned predominantly on microvilli, and CCL was found on the cell body at a degree similar to the respective wild types (Fig. 2).

The Transmembrane Domain Governs Receptor Surface Presentation—The unchanged distributions of LLC and CCL compared with LLL and CCC suggest that the motif for the surface localization of L-selectin and CD44 may be encoded in their outer segments. Previous work had established that swapping the EC domains alone had no effect (4). We confirmed this finding because the chimera LCC remained on the planar cell

Downloaded from www.jbc.org at Biomedical Library, UCSD, on September 30, 2010

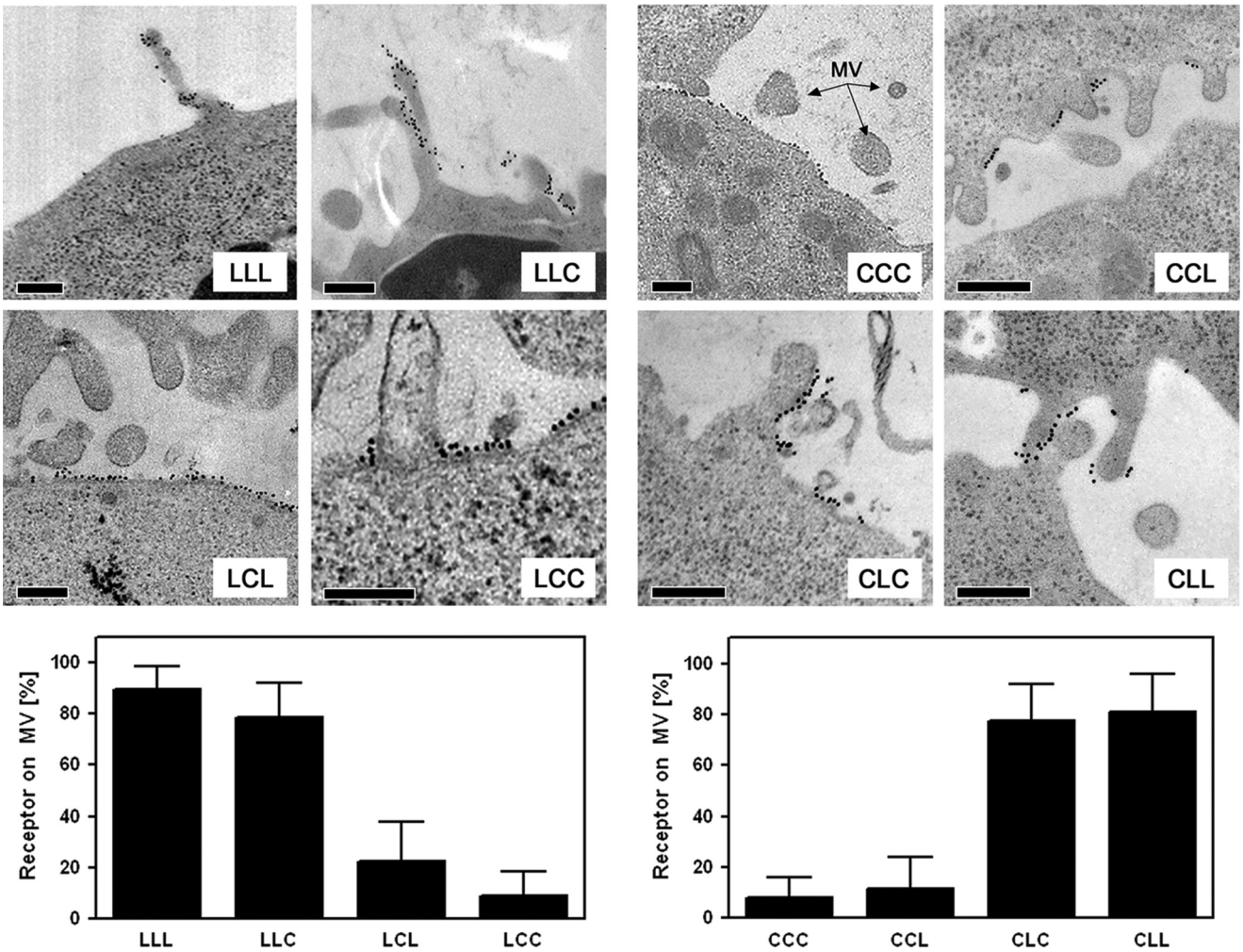

FIGURE 2. **Receptor cell surface topography of K562 transfectants.** Human wild type L-selectin, CD44, or chimeric receptors expressed by transfected K562 cells were analyzed for their surface localization. Using immunogold labeling and transmission electron microscopy, all 10-nm gold particles (*black dots*) were categorized as cell body- or microvillus (*MV*)-based. Representative surface patterns ($n = 2$ in duplicate) with their receptor distribution on microvilli of L-selectin transfectants (*left*) and CD44-transfectants (*right*) are shown. Data are presented as mean ± S.D. (*error bars*). LCL expression is about half as high as LLL, LLC, and LCC. 20–30 cells with a total of ~700–1,400 gold particles were counted for each experiment. *Scale bars*, 0.1 μm.

body and CLL was expressed on microvilli in a ratio similar to CCC and LLL, respectively (Fig. 2). These findings in conjunction with the result that swapping of the IC domain did not have significant effects on cell surface topology suggest that the TM domain may be a major determinant of L-selectin and CD44 surface presentation.

To examine this hypothesis, we generated chimeras with a replaced TM but unmodified IC and EC segment (Fig. 1*A*). Indeed, substitution of the L-selectin TM domain (LCL) provoked a significant loss of the microvillus localization, with 80% of all labeled proteins found on the planar cell body and excluding microvilli (Fig. 2), similar to CD44 typical surface distribution. Likewise, CLC was hardly found on the planar cell body but showed a major shift to the microvillus compartment.

Domain Swapping Does Not Alter Static Adhesion—To address the functional implications of surface localization, we established cell transfectants with tightly matched surface expression levels, which was successful for all constructs except LCL (Fig. 1, *C* and *D*). Static binding of wild type L-selectin and chimeras was assessed using immobilized PSGL-1, a known ligand for L-selectin (28). Cells were allowed to settle on coated hydrophobic glass slides, and the number of bound cells was counted. No significant difference in binding activity between the N-terminal ligand-binding lectin domains of L-selectin wild type and chimeras could be detected (Fig. 3*A*). Similarly, the static adhesion activity of the CD44 transfectants was investigated using its physiologic ligand hyaluronan (29), showing no evidence for differential adhesion (Fig. 3*B*).

Microvillus Receptor Presentation Enhances Adhesion under Flow—L-selectin supports fast leukocyte rolling on PSGL-1 (30), whereas CD44 mediates very slow rolling on hyaluronan (29). Therefore, we used clones with similar surface expression levels to assess rolling flux and velocity for all L-selectin assays and cell accumulation for CD44 assays, respectively. To mimic leukocyte-endothelium interactions, a parallel plate flow chamber was used, allowing the characterization of the adhesion behavior under defined wall shear stress conditions.

L-selectin showed efficient tethering and subsequent rolling at shear stresses between 0.7 and 2.3 dynes/cm^2. Both mock transfectants and the blocking anti-L-selectin mAb DREG-200 were employed as specificity controls and completely abolished all interaction. Consistent with published data (4), the cell

Downloaded from www.jbc.org at Biomedical Library, UCSD, on September 30, 2010

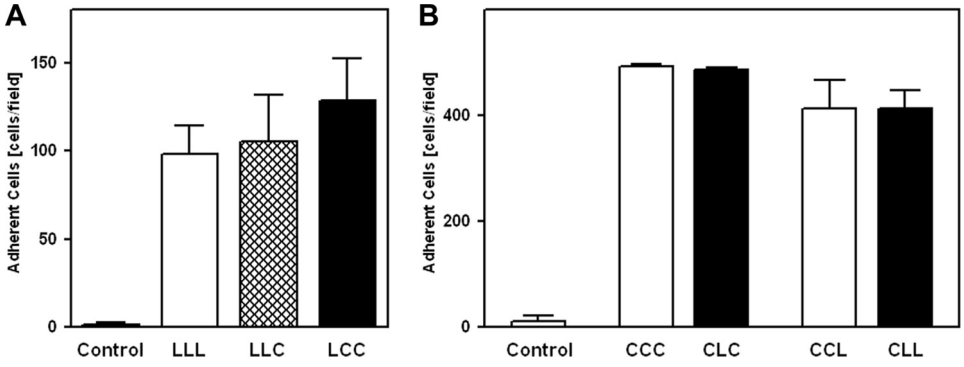

FIGURE 3. **Static adhesion of K562 transfectants.** *A*, static binding of L-selectin transfectants to immobilized PSGL-1 on hydrophobic glass slides. The specificity of binding was confirmed by cells preincubated with blocking DREG-200 mAb (*Control*). Mean ± S.D. (*error bars*) of five independent experiments are shown. *B*, CD44 cell transfectants bound to hyaluronan under static conditions. Blocking anti-CD44 mAb served as control. CCC and CLC express closely matched surface expression levels, as do CCL and CLL. Data are presented as mean ± S.D. of three independent experiments.

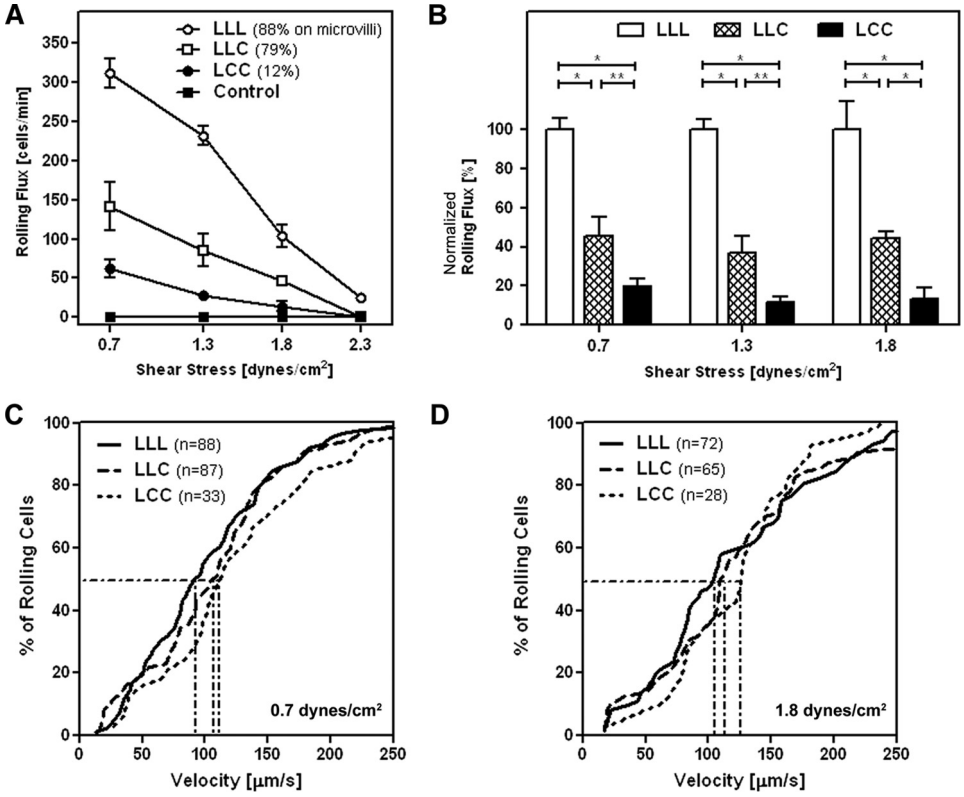

FIGURE 4. **Rolling of L-selectin transfectants on PSGL-1.** K562 cells transfected with L-selectin wild type (LLL) and chimeras LLC and LCC rolling on PSGL-1 under different shear conditions are shown. The compared cell lines shared a similar surface expression level (Fig. 1). *A*, steady-state rolling flux. Cells incubated with the blocking anti-human DREG-200 mAb served as negative control. Data are presented as mean ± S.D. (*error bars*) of five independent experiments. *B*, same data, but normalized to rolling flux of LLL (=100%). *, $p < 0.002$; **, $p < 0.015$ (paired *t* test, $n = 5$ in each group). *C* and *D*, cumulative velocity histograms of L-selectin transfectants at 0.7 (*C*) and 1.8 (*D*) dynes/cm^2. *n* indicates the number of rolling cells analyzed.

body-based chimera LCC showed a severely reduced rolling flux compared with microvillus-expressed LLL. LLC showed an intermediate phenotype between LLL and LCC at all tested shear rates (Fig. 4, *A* and *B*). The rolling velocity of LLL, LCC, and LLC was similar under all conditions (Fig. 4, *C* and *D*). Detailed data are provided in Table 1.

Next, we investigated whether microvillus positioning can improve the cell adhesion function of CD44. Expression-matched pairs of CCC and CLC as well as CLL and CCL, respectively, were compared in a flow chamber assay (Fig. 5). In both cases, microvillus-expressed CD44 receptors (CLC, CLL) supported ~3-fold more adhesion than the cell body-based counterparts. Note that both pairs contain the same cytoplasmic tail and thus have the same intracellular anchorage.

DISCUSSION

In this study, the impact of the EC, TM, and IC domain of L-selectin and CD44 on adhesion receptor surface positioning and functionality was evaluated to clarify puzzling data concerning the contribution of the cytoplasmic anchorage of L-selectin and CD44. Using electron microscopy, no significant impact of the IC tail could be detected for both molecules, suggesting that receptor surface pattern is not determined by cytoplasmic interactions. However, mutations of ERM-binding residues within the proximal IC domain of L-selectin are known to abolish expression on microvilli (20), but deleting its distal cytoplasmic tail does not (21), consistent with both L-selectin and CD44 being constitutively ERM-associated (22). Therefore, ERM linkage of compartmentalized cell surface receptors seems to be necessary but not sufficient for defining their sorting to microvilli or the cell body. Further domain swapping revealed the TM domain to be a key determinant of receptor surface compartmentalization irrespective of the EC and IC domains.

In polarized cells, selective targeting and intracellular stabilization at the basolateral and apical cell surface are two putative mechanisms responsible for cell polarization enabling biochemically and functionally distinct plasma membrane domains (31). Epithelial cells are microvilli-bearing on their apical site whereas the basolateral compartment remains rather flat, resembling the protrusive and flat subdomains on leukocytes. Receptors of blood-borne nonpolarized cells may be compartmentalized by a cognate sorting machinery (32). Given our findings, it seems that leukocyte receptor compartmentalization involves two functionally separate processes: selective targeting via the TM domain and perhaps stabilization through ERM linkage present in both CD44 and L-selectin. The

Downloaded from www.jbc.org at Biomedical Library, UCSD, on September 30, 2010

TABLE 1

Rolling of K562 transfectants on recombinant PSGL-1

L-selectin wild type and chimeras rolling on PSGL-1 at low, medium, and high shear stress are shown. Rolling flux data include five independent experiments. *n* indicates the number of cells analyzed for rolling velocity.

Shear stress	Receptor	Rolling flux mean ± S.D.[a]	Rolling velocity		
			Mean ± S.D.[b]	Median	*n*
dynes/cm²		*cells/min*	*μm/s*	*μm/s*	
0.7	LLL	312 ± 18	103 ± 58	93	88
	LLC	142 ± 30[c]	107 ± 58	109	87
	LCC	62 ± 12[c]	120 ± 56	112	33
1.3	LLL	232 ± 12	116 ± 67	113	75
	LLC	85 ± 21[d]	117 ± 59	111	71
	LCC	27 ± 6[c]	133 ± 67	126	29
1.8	LLL	104 ± 15	119 ± 70	104	72
	LLC	46 ± 4[c]	131 ± 80	115	65
	LCC	14 ± 6[c]	138 ± 46	131	28

[a] Cells during steady-state rolling crossing a virtual perpendicular line of 1-mm length within 1 min.
[b] The velocity of steadily rolling cells was analyzed using a MATLAB snake model tracking algorithm.
[c] $p < 0.002$ compared with LLL (paired *t* test); $n = 5$ at each condition.
[d] $p < 0.015$ compared with LLL (paired *t* test); $n = 5$ at each condition.

ERM-binding residues and TM domains are highly conserved in mammals, supporting a close functional link (Fig. 6).

As a precondition for functional flow assays, the ability of the constructs to bind ligand was compared in a static environment. Neither receptor surface topology nor domain swapping influenced the adhesive function of L-selectin or CD44 (Fig. 3). Under flow, however, a significant effect on adhesion could be detected at all tested shear levels. At 0.7 and 1.8 dynes/cm^2, the rolling flux of LLC was approximately 45% of that of LLL. LCC supported about 20% of the rolling flux of LLL at 0.7 dynes/cm^2 and about 12% at higher shear stress (Fig. 4*B*), suggesting that differential attachment rates favored by microvillus-expressed receptors become more obvious at increasing shear. However, rolling velocity is not a function of either the topographic distribution (17) or of specific cytoplasmic anchorage. This is consistent with the hypothesis that receptor off-rate, determined by the EC domain, determines rolling velocity (33).

Defective tethering may be caused by the missing cytoplasmic α-actinin binding site that was shown to play a central role in leukocyte tethering under flow (21, 34). Indeed, the substitution of the L-selectin IC domain (LLC) primarily evoked a dramatic loss in initiating adhesion under flow (Fig. 4) but did not change surface distribution (Fig. 2). Moreover, receptor presentation on microvilli is sufficient for increased adhesion under physiologic shear conditions as shown by LLC (on microvilli) compared with LCC (on the cell body; Fig. 4, *A* and *B*). These results are further supported by reciprocal experiments using CD44 chimeras. Both microvillus-expressed constructs containing the TM domain of L-selectin (CLC, CLL) showed superior adhesion compared with their cell body-expressed counterparts under flow (Fig. 5) but not under static conditions (Fig. 3*B*). Thus, the strong enhancement of CD44 adhesion under flow through the introduction of the L-selectin TM segment is likely to be a functional consequence of the receptor shift from the cell body to microvilli. Together, these findings emphasize that the TM domain is responsible for specific receptor surface positioning with direct consequences on receptor functionality.

The CD44 and L-selectin TM domains are both 95–100% conserved among mammalian species (Fig. 6). Our data are the first to demonstrate that these TM helices indeed take

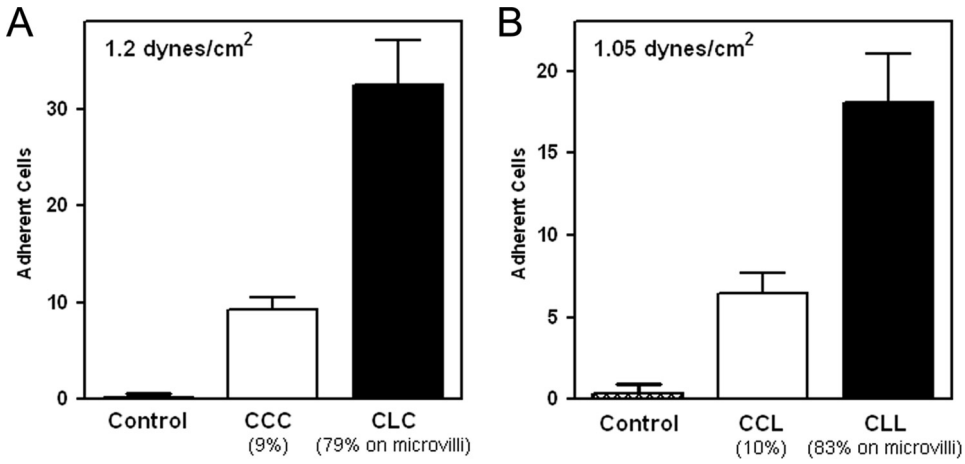

FIGURE 5. **Accumulation of CD44 transfectants on hyaluronan under flow.** Rolling and adherent K562 cells transfected with wild type or chimeric CD44 were counted 7 min after the initiation of flow within a field of 1 mm^2 in a flow chamber setup. Each pair of cell lines shared a similar receptor surface expression level (Fig. 1). Accumulation of mock transfectants (*Control*) was negligible. All *bars* show mean ± S.D. (*error bars*) of three independent experiments.

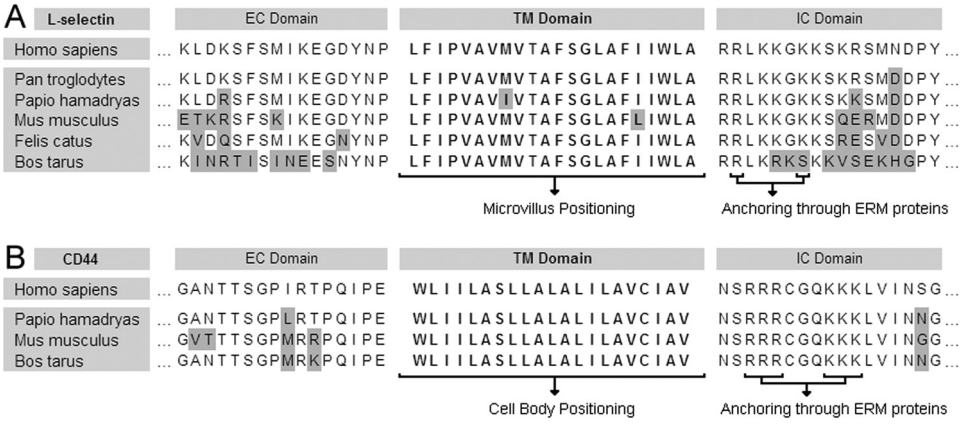

FIGURE 6. **Phylogenetic comparison of L-selectin and CD44 membrane-spanning regions.** Primary amino acid sequences of different species are depicted with their predicted IC and TM domains along with the adjacent beginning of the EC segment. Single amino acids differing from *Homo sapiens* are *highlighted gray*. The *vertical order* roughly reflects the taxonomic distance to *H. sapiens* (from *top* to *bottom*). ERM-binding residues are indicated according to Refs. 20 and 22. For multiple sequence alignment, the program ClustalW2 was used with default settings.

Downloaded from www.jbc.org at Biomedical Library, UCSD, on September 30, 2010

center stage in physiologic receptor function by defining surface localization. E-selectin, another member of the selectin family, is displayed ubiquitously on the surface of pre-B cell transfectants, including flat and protrusive sections (4). Despite the close relationship to L-selectin in the EC domain, its TM domain is barely conserved in mammals. Thus, it is plausible to propose that noncompartmentalization of leukocyte surface receptors constitutes a "default pathway," whereas TM signals lead to an active segregation to the cell body or microvilli.

Research about the organization of the plasma membrane has focused on cholesterol-enriched microdomains (lipid rafts) as a main constituent of distinct subdomains. The tyrosine kinase $p56^{Lck}$ was shown to play a central role in trafficking the CD4 receptor to microvilli in the lymphoid cell line CEM (35). Notably, lymphocyte L-selectin requires functional $p56^{Lck}$ for the activation of the Ras pathway (36). Moreover, a PSGL-1 mutant lacking the IC tail and thus missing a putative ERM binding domain still concentrates on microvilli of primary leukocytes (6). Because this mutant was still able to associate with lipid rafts and promote normal rolling on P-selectin, the authors hypothesized that cytoskeletal anchorage of PSGL-1 was achieved through raft molecules that, in turn, link to actin. Similarly, the deletion of the C-terminal tail of prominin, a pentaspan TM glycoprotein associated with lipid rafts, does not perturb its accumulation on microvilli (37). Collectively, these findings support the concept of lipid raft integrity as a precondition for microvillus receptor presentation. However, other studies seem to contradict: cell body CD44 in murine fibroblasts (38) but not microvillus L-selectin in human primary cells (39) was shown to be enriched in rafts using the detergent Triton X-100. This incongruence could be due to cell type-specific discrepancies, the existence of multiple mechanisms for protein sorting, or multiple types of rafts populating different surface subdomains.

The complexity of microvillus receptor expression is illustrated by the failure of transfected K562 cells to display human wild type PSGL-1 on microvilli (40) unlike primary cells (7, 6). This points to possible accessory molecules necessary for PSGL-1 but not L-selectin positioning. Similarly, the CD44 receptor localizes to the planar cell body of L1–2 pre-B cells (4), but not of a melanoma cell line (22). Furthermore, domain swapping experiments of α4- and β2-integrins (on microvilli and on the cell body, respectively) suggest that EC interactions may be responsible for microvillus positioning (41). Taken together, despite a very similar phenotype, the underlying mechanisms for the association of different surface receptors with microvilli seem to be diverse. Cytoskeletal anchorage, EC and TM interactions, as well as lipid raft integrity appear to contribute to a microvillus expression pattern. However, the surface expression patterns of CD44 and L-selectin are determined by the TM domain.

Membrane-spanning domains not only function as membrane anchors but also play a critical role in receptor functionality (42, 43). Through lateral membrane interactions or dynamic conformational changes, TM domains are known to regulate the formation of heterogeneous protein complexes and protein folding, yet there is to date no evidence about any particular impact on receptor localization. The biological importance is highlighted by several disease-associated mutations within single-spanning TM domains clinically leading to severe pathologies such as achondroplasia, acute myeloid leukemia, or lupus (43). Because the extent of microvilli on cancer cells is correlated with the hematogenous dissemination potential of the tumor (44), our findings suggest that TM domains of adhesion receptors may also play a role in metastasis. Insights about the physiology of TM interactions can therefore guide studies into new therapeutic targets in inflammation and cancer metastasis.

Acknowledgment—We thank Dr. Andrea Löwendorf for the critical evaluation of this manuscript.

REFERENCES

1. Springer, T. A. (1994) *Cell* **76,** 301–314
2. Ley, K., Laudanna, C., Cybulsky, M. I., and Nourshargh, S. (2007) *Nat. Rev. Immunol.* **7,** 678–689
3. Dow, L. E., and Humbert, P. O. (2007) *Int. Rev. Cytol.* **262,** 253–302
4. von Andrian, U. H., Hasslen, S. R., Nelson, R. D., Erlandsen, S. L., and Butcher, E. C. (1995) *Cell* **82,** 989–999
5. Berlin, C., Bargatze, R. F., Campbell, J. J., von Andrian, U. H., Szabo, M. C., Hasslen, S. R., Nelson, R. D., Berg, E. L., Erlandsen, S. L., and Butcher, E. C. (1995) *Cell* **80,** 413–422
6. Miner, J. J., Xia, L., Yago, T., Kappelmayer, J., Liu, Z., Klopocki, A. G., Shao, B., McDaniel, J. M., Setiadi, H., Schmidtke, D. W., and McEver, R. P. (2008) *Blood* **112,** 2035–2045
7. Bruehl, R. E., Moore, K. L., Lorant, D. E., Borregaard, N., Zimmerman, G. A., McEver, R. P., and Bainton, D. F. (1997) *J. Leukocyte Biol.* **61,** 489–499
8. Singer, I. I., Scott, S., Kawka, D. W., Chin, J., Daugherty, B. L., DeMartino, J. A., DiSalvo, J., Gould, S. L., Lineberger, J. E., Malkowitz, L., Miller, M. D., Mitnaul, L., Siciliano, S. J., Staruch, M. J., Williams, H. R., Zweerink, H. J., and Springer, M. S. (2001) *J. Virol.* **75,** 3779–3790
9. Erlandsen, S. L., Hasslen, S. R., and Nelson, R. D. (1993) *J. Histochem. Cytochem.* **41,** 327–333
10. Hocdé, S. A., Hyrien, O., and Waugh, R. E. (2009) *Biophys. J.* **97,** 379–387
11. Arbonés, M. L., Ord, D. C., Ley, K., Ratech, H., Maynard-Curry, C., Otten, G., Capon, D. J., and Tedder, T. F. (1994) *Immunity* **1,** 247–260
12. Siegelman, M. H., DeGrendele, H. C., and Estess, P. (1999) *J. Leukocyte Biol.* **66,** 315–321
13. Hanley, W. D., Napier, S. L., Burdick, M. M., Schnaar, R. L., Sackstein, R., and Konstantopoulos, K. (2006) *FASEB J.* **20,** 337–339
14. H., Stevenson, J. L., Varki, A., Varki, N. M., and Borsig, L. (2006) *Cancer Res.* **66,** 1536–1542
15. Von Andrian, U. H., Hansell, P., Chambers, J. D., Berger, E. M., Torres Filho, I., Butcher, E. C., and Arfors, K. E. (1992) *Am. J. Physiol. Heart Circ. Physiol.* **263,** H1034–H1044
16. Ley, K., Bullard, D. C., Arbonés, M. L., Bosse, R., Vestweber, D., Tedder, T. F., and Beaudet, A. L. (1995) *J. Exp. Med.* **181,** 669–675
17. Stein, J. V., Cheng, G., Stockton, B. M., Fors, B. P., Butcher, E. C., and von Andrian, U. H. (1999) *J. Exp. Med.* **189,** 37–50
18. Chhabra, E. S., and Higgs, H. N. (2007) *Nat. Cell Biol.* **9,** 1110–1121
19. Bonifacino, J. S., and Traub, L. M. (2003) *Annu. Rev. Biochem.* **72,** 395–447
20. Ivetic, A., Florey, O., Deka, J., Haskard, D. O., Ager, A., and Ridley, A. J. (2004) *J. Biol. Chem.* **279,** 33263–33272
21. Pavalko, F. M., Walker, D. M., Graham, L., Goheen, M., Doerschuk, C. M., and Kansas, G. S. (1995) *J. Cell Biol.* **129,** 1155–1164
22. Legg, J. W., and Isacke, C. M. (1998) *Curr. Biol.* **8,** 705–708
23. Walcheck, B., Moore, K. L., McEver, R. P., and Kishimoto, T. K. (1996) *J. Clin. Invest.* **98,** 1081–1087
24. Kansas, G. S., Wood, G. S., and Dailey, M. O. (1989) *J. Immunol.* **142,** 3050–3057
25. Cannistra, S. A., Kansas, G. S., Niloff, J., DeFranzo, B., Kim, Y., and Ottens-

Downloaded from www.jbc.org at Biomedical Library, UCSD, on September 30, 2010

meier, C. (1993) *Cancer Res.* **53,** 3830–3838
26. Horton, R. M., Hunt, H. D., Ho, S. N., Pullen, J. K., and Pease, L. R. (1989) *Gene* **77,** 61–68
27. Shakibaei, M., Zimmermann, B., and Scheller, M. (1993) *J. Struct. Biol.* **111,** 180–189
28. Spertini, O., Cordey, A. S., Monai, N., Giuffrè, L., and Schapira, M. (1996) *J. Cell Biol.* **135,** 523–531
29. DeGrendele, H. C., Estess, P., Picker, L. J., and Siegelman, M. H. (1996) *J. Exp. Med.* **183,** 1119–1130
30. Sperandio, M., Smith, M. L., Forlow, S. B., Olson, T. S., Xia, L., McEver, R. P., and Ley, K. (2003) *J. Exp. Med.* **197,** 1355–1363
31. Matter, K. (2000) *Curr. Biol.* **10,** R39–R42
32. Matter, K., and Mellman, I. (1994) *Curr. Opin. Cell Biol.* **6,** 545–554
33. Krasik, E. F., and Hammer, D. A. (2004) *Biophys. J.* **87,** 2919–2930
34. Kansas, G. S., Ley, K., Munro, J. M., and Tedder, T. F. (1993) *J. Exp. Med.* **177,** 833–838
35. Foti, M., Phelouzat, M. A., Holm, A., Rasmusson, B. J., and Carpentier, J. (2002) *Proc. Natl. Acad. Sci. U.S.A.* **99,** 2008–2013
36. Brenner, B., Gulbins, E., Schlottmann, K., Koppenhoefer, U., Busch, G. L., Walzog, B., Steinhausen, M., Coggeshall, K. M., Linderkamp, O., and Lang, F. (1996) *Proc. Natl. Acad. Sci. U.S.A.* **93,** 15376–15381
37. Corbeil, D., Röper, K., Hannah, M. J., Hellwig, A., and Huttner, W. B. (1999) *J. Cell Sci.* **112,** 1023–1033
38. Perschl, A., Lesley, J., English, N., Hyman, R., and Trowbridge, I. S. (1995) *J. Cell Sci.* **108,** 1033–1041
39. Dwir, O., Grabovsky, V., Pasvolsky, R., Manevich, E., Shamri, R., Gutwein, P., Feigelson, S. W., Altevogt, P., and Alon, R. (2007) *J. Immunol.* **179,** 1030–1038
40. Snapp, K. R., Craig, R., Herron, M., Nelson, R. D., Stoolman, L. M., and Kansas, G. S. (1998) *J. Cell Biol.* **142,** 263–270
41. Abitorabi, M. A., Pachynski, R. K., Ferrando, R. E., Tidswell, M., and Erle, D. J. (1997) *J. Cell Biol.* **139,** 563–571
42. Li, X., Pérez, L., Pan, Z., and Fan, H. (2007) *Cell Res.* **17,** 985–998
43. Moore, D. T., Berger, B. W., and DeGrado, W. F. (2008) *Structure* **16,** 991–1001
44. Azuma, H., Takahara, S., Ichimaru, N., Wang, J. D., Itoh, Y., Otsuki, Y., Morimoto, J., Fukui, R., Hoshiga, M., Ishihara, T., Nonomura, N., Suzuki, S., Okuyama, A., and Katsuoka, Y. (2002) *Cancer Res.* **62,** 1410–1419

Downloaded from www.jbc.org at Biomedical Library, UCSD, on September 30, 2010